Inorganic Chemistry

Article

Template-Assisted Synthesis of Shape-Controlled Rh$_2$P Nanocrystals

Amanda E. Henkes[†] and Raymond E. Schaak*,[†,‡]

Departments of Chemistry, Texas A&M University, P.O. Box 30012, College Station, Texas 77842, and The Pennsylvania State University, 104 Chemistry Building, University Park, Pennsylvania 16802

When reacted with trioctylphosphine at ∼360 °C, rhodium nanocrystals convert to rhodium phosphide (Rh$_2$P) nanocrystals. Careful control over synthetic variables, such as temperature, stabilizing ligands, and cosolvents, can result in Rh$_2$P nanocrystals with shapes that reflect the Rh nanocrystal templates. Accordingly, Rh nanocrystals with multipod, cube- and triangle-derived shapes convert to Rh$_2$P nanocrystals that maintain the shape of their Rh precursors. Both dense and hollow Rh$_2$P nanocrystals can be generated using a single unified chemical conversion strategy. These empirical guidelines for generating a morphologically diverse library of Rh$_2$P nanocrystals provide important insights into shape conservation using nanocrystal templates and will likely be portable to other multielement systems for which rigorous shape-controlled synthesis remains challenging.

Introduction

Because of quantum effects in nanocrystals[1] and the differences in properties between nanoscale and bulk materials,[2] the development of simple, efficient, and general methods for nanocrystal synthesis is becoming increasingly important. In particular, the interesting changes in the properties of nanoscale materials relative to their bulk analogues are often linked to the shape and morphology of the nanocrystals.[2,3] As a result, understanding and fine-tuning the synthetic variables that induce shape control in nanocrystals can allow one to control the properties of a material, for example in catalysis[4] and optics.[5,6] While there exist a growing number of well-controlled methods for synthesizing metal nanocrystals with precise sizes and shapes (i.e., nanorods, nanocubes, and tetrapods), most are only applicable for single-metal systems[7,8] and some simple binary and alloy phases.[9] Expanding and generalizing these synthetic capabilities to more complex multielement systems, which is necessary for developing advanced applications and studying size–shape–structure–property interrelationships in exotic nanoscale solids, remains a significant challenge. In particular, generating high-quality multielement nanocrystals requires that several key issues be simultaneously addressed, including availability of appropriate soluble precursors, kinetics of precursor reduction or decomposition, conucle-

* To whom correspondence should be addressed. E-mail: schaak@chem.psu.edu.
† Texas A&M University.
‡ The Pennsylvania State University.
(1) Alivisatos, A. P. *Science* **1996**, *271*, 933−937.
(2) El-Sayed, M. A. *Acc. Chem. Res.* **2004**, *37*, 326−333.
(3) (a) Scher, E. K.; Manna, L.; Alivisatos, A. P. *Philos. Trans. R. Soc. London, Ser. A* **2003**, *361*, 241−257. (b) Burda, C.; Chen, X.; Narayanan, R.; El-Sayed, M. A. *Chem. Rev.* **2005**, *105*, 1025−1102.
(4) (a) Narayana, R.; El-Sayed, M. A. *Nano Lett.* **2004**, *4*, 1343−1348. (b) Daniel, M.-C.; Astruc, D. *Chem. Rev.* **2004**, *104*, 293−346. (c) Tian, N.; Zhou, Z.-Y.; Sun, S.-G.; Ding, Y.; Wang, Z. L. *Science* **2007**, *316*, 732−735.
(5) (a) Chen, J.; Wiley, B.; Li, Z.-Y.; Campbell, D.; Saeki, F.; Cang, H.; Au, L.; Lee, J.; Li, X.; Xia, Y. *Adv. Mater.* **2005**, *17*, 2255−2261. (b) Eustis, S.; El-Sayed, M. A. *Chem. Soc. Rev.* **2006**, *35*, 209−217.
(6) (a) Li, L.-S.; Hu, J.; Yang, W.; Alivisatos, A. P. *Nano Lett.* **2001**, *1*, 349−351. (b) Murphy, C. J.; Sau, T. K.; Gole, A. M.; Orendorff, C. J.; Gau, J.; Gou, L.; Hunyadi, S. E.; Li, T. *J. Phys. Chem. B* **2005**, *109*, 13857−13870. (c) Orendorff, C. J.; Gole, A.; Sau, T. K.; Murphy, C. J. *Anal. Chem.* **2005**, *77*, 3261−3266.

(7) (a) Wiley, B.; Sun, Y.; Mayers, B.; Xia, Y. *Chem.—Eur. J.* **2005**, *11*, 454−463. (b) Kim, F.; Connor, S.; Song, H.; Kuykendall, T.; Yang, P. *Angew. Chem., Int. Ed.* **2004**, *43*, 3673−3677. (c) Sun, Y.; Xia, Y. *Science* **2002**, *298*, 2176−2179. (d) Xiong, Y.; McLellan, J. M.; Yin, Y.; Xia, Y. *Angew. Chem., Int. Ed.* **2007**, *46*, 790−794. (e) Washio, I.; Xiong, Y.; Yin, Y.; Xia, Y. *Adv. Mater.* **2006**, *18*, 1745−1749. (f) Wiley, B. J.; Xiong, Y.; Li, Z.-Y.; Yin, Y.; Xia, Y. *Nano Lett.* **2006**, *6*, 765−768. (g) Xiong, Y.; Washio, I.; Chen, J.; Cai, H.; Li, Z.-Y.; Xia, Y. *Langmuir* **2006**, *22*, 8563−8570. (h) Seo, D.; Park, J. C.; Song, H. *J. Am. Chem. Soc.* **2006**, *128*, 14863−14870.
(8) (a) Berhault, G.; Bausach, M.; Bisson, L.; Becerra, L.; Thomazeau, C.; Uzio, D. *J. Phys. Chem. C* **2007**, *111*, 5915−5925. (b) Sau, T. K.; Murphy, C. J. *J. Am. Chem. Soc.* **2004**, *126*, 8648−8649. (c) Chen, S.; Wang, Z. L.; Ballato, J.; Foulger, S. H.; Carroll, D. L. *J. Am. Chem. Soc.* **2003**, *125*, 16186−16187.
(9) (a) Lee, S.-M.; Cho, S.-N.; Cheon, J. *Adv. Mater.* **2003**, *15*, 441−444. (b) Peng, X. *Adv. Mater.* **2003**, *15*, 459−463. (c) Mana, L.; Scher, E. C.; Alivisatos, A. P. *J. Am. Chem. Soc.* **2000**, *122*, 12700−12706. (d) Chen, J.; McLellen, J. M.; Siekkinen, A.; Xiong, Y.; Li, Z.-Y.; Xia, Y. *J. Am. Chem. Soc.* **2006**, *128*, 14776−14777. (e) Maksimuk, S.; Yang, S.; Peng, Z.; Yang, H. *J. Am. Chem. Soc.* **2007**, *129*, 8684−8685.

ation of the elements into the desired phase, and controllable anisotropic growth (for shape control).[10−12] These issues, and the interplay among them, often make it difficult to readily apply the concepts developed for the shape-controlled synthesis of single-metal nanocrystals to even the simplest multimetal systems.

Recognizing these challenges, a straightforward strategy for minimizing these synthetic complexities is to use single-metal nanocrystals as reactive templates that convert to a desired multimetal phase while retaining the morphology of the single-metal nanoparticle precursor. Because there are many methods for forming metal nanocrystals,[7−8,10−13] they can serve as readily available reagents for conversion into more complex materials. This approach has been used quite successfully to generate metal selenide nanowires,[14] silver iodide nanoplatelets,[15] and hollow nanostructures of metal sulfides,[16−17] selenides,[16,18] oxides,[16] and late transition metal alloys.[19] Our group has been expanding this strategy to more complex solids, such as multimetal intermetallic compounds[20−23] and transition metal phosphides.[24,25] For example, our group[24,25] and the Chiang group[26] have both recently shown that metal nanocrystals react with hot trioctylphosphine (TOP) to form metal phosphides. These investigations suggest that the size and shape of the metal nanoparticle precursor can influence the shape of the metal phosphide product.

While there are several reports describing the synthesis of high-quality, single-crystal metal phosphide nanorods and wires,[27−32] the anisotropic growth is influenced by the

stabilizers present and the constant supply of an organometallic−phosphine complex feedstock, which is not easily modified to create more complex and varied morphologies using standard one-pot reactions. This is in contrast to many single-metal systems, which can be made to form a variety of elaborate shapes that include rods, cubes, octahedra, tetrahedra, icosahedra, tetrapods, bipyramids, triangular and hexagonal nanoplates, belts, and hollow derivatives.[6b,7,8] Here we report the synthesis of rhodium phosphide (Rh_2P) nanocrystals with a variety of complex morphologies, including cubes, triangles, and multipods. This represents the most morphologically diverse library of metal phosphide nanocrystals reported to date. Importantly, these morphologies have not been reported for *any* metal phosphide nanocrystals yet are straightforward to access using existing shape-controlled metal nanocrystals as templates. Furthermore, we show that these nanocrystal shapes can be made hollow by exploiting a Kirkendall mechanism.[16,24,26] Finally, we establish the critical role that surface stabilizers have on allowing a metal nanocrystal to be transformed, in a shape-retaining manner, into a metal phosphide nanocrystal.

Our prototype system for these studies, Rh/Rh_2P, was chosen for several reasons. As a metal nanoparticle template for inducing shape control in a derivative system, Rh is ideal since it is possible to synthesize Rh nanocrystals in a variety of elaborate shapes.[33−37] While other metal phosphide systems are more technologically relevant and have been studied in more detail (e.g., MnP, FeP, InP, and Ni_2P),[27−28,38−39] the corresponding metal nanocrystal precursors tend to not be as readily available in the diversity of shapes reported for Rh. This allows Rh/Rh_2P to serve as the most useful model system for studying shape-controlled metal/phosphide conversions. Our prior studies have shown that spherical Rh nanoparticles convert cleanly to Rh_2P upon reaction with hot TOP.[24] Thus, the conversion reaction for this system is robust and therefore is ideal for applying to more complex nanocrystal morphologies such as those achievable for Rh. Finally,

(10) Cushing, B. L.; Kolesnichenko, V. L.; O' Connor, C. J. *Chem. Rev.* **2004**, *104*, 3893−3946.

(11) (a) Jun, Y.-W.; Choi, J.-S.; Cheon, J. *Angew. Chem., Int. Ed.* **2006**, *45*, 3414−3439. (b) Park, J.; Joo, J.; Kwon, S. G.; Jang, Y.; Hyeon, T. *Angew. Chem., Int. Ed.* **2007**, *46*, 4630−4660. (c) Hyeon, T. *Chem. Commun.* **2003**, 927−934.

(12) Jun, Y.-W.; Lee, J.-H.; Choi, J.-S.; Cheon, J. *J. Phys. Chem. B* **2005**, *109*, 14795−14806.

(13) (a) Kurihara, L. K.; Chow, G. M.; Shoen, P. E. *NanoStruct. Mater.* **1995**, *5*, 607−613. (b) Green, M. *Chem. Commun.* **2005**, 3002−3011. (c) Wang, X.; Zhuang, J.; Peng, Q.; Li, Y. *Nature* **2005**, *437*, 121−124.

(14) (a) Gates, B.; Wu, Y.; Yin, Y.; Yang, P.; Xia, Y. *J. Am. Chem. Soc.* **2001**, *123*, 11500−11501. (b) Gates, B.; Mayers, B.; Wu. Y.; Sun, Y.; Cattle, B.; Yang, P.; Xia, Y. *Adv. Funct. Mater.* **2002**, *12*, 679−686.

(15) Ng, C. H. B.; Fan, W. Y. *J. Phys. Chem. C* **2007**, *111*, 2953−2958.

(16) Yin, Y.; Rioux, R. M.; Erdonmez, C. K.; Hughes, S.; Somorjai, G. A.; Alivisatos, A. P. *Science* **2004**, *304*, 711−714.

(17) Yin, Y.; Erdonmez, C. K.; Cabot, A.; Hughes, S.; Alivisatos, A. P. *Adv. Funct. Mater.* **2006**, *16*, 1389−1399.

(18) Tan, H.; Li, S.; Fan, W. Y. *J. Phys. Chem. B* **2006**, *110*, 15812−15816.

(19) (a) Sun, Y.; Wiley, B.; Li, Z.-H.; Xia, Y. *J. Am. Chem. Soc.* **2004**, *126*, 9399−9406. (b) Vasquez, Y.; Sra, A. K.; Schaak, R. E. *J. Am. Chem. Soc.* **2005**, *127*, 12504−12505.

(20) Cable, R. E.; Schaak, R. E. *J. Am. Chem. Soc.* **2006**, *128*, 9588−9589.

(21) Leonard, B. M.; Schaak, R. E. *J. Am. Chem. Soc.* **2006**, *128*, 11475−11482.

(22) Chou, N. H.; Schaak, R. E. *J. Am. Chem. Soc.* **2007**, *129*, 7339−7345.

(23) Cable, R. E.; Schaak, R. E. *Chem. Mater.* **2007**, *19*, 4098−4104.

(24) Henkes, A. E.; Vasquez, Y.; Schaak, R. E. *J. Am. Chem. Soc.* **2007**, *129*, 1896−1897.

(25) Henkes, A. E.; Schaak, R. E. *Chem. Mater.* **2007**, *19*, 4234−4242.

(26) Chiang, R.-K.; Chiang, R.-T. *Inorg. Chem.* **2007**, *46*, 369−371.

(27) Gregg, K. A.; Perera, S. C.; Lawes, G.; Shinozaki, S.; Brock, S. L. *Chem. Mater.* **2006**, *18*, 879−886.

(28) Park, J.; Koo, B.; Yoon, K. Y.; Hwang, Y.; Kang, M.; Park, J.-G.; Hyeon, T. *J. Am. Chem. Soc.* **2005**, *127*, 8433−8440.

(29) Li, Y.; Malik, M. A.; O'Brien, P. *J. Am. Chem. Soc.* **2005**, *127*, 16020−16021.

(30) Qian, C.; Kim, F.; Ma, L.; Tsui, F.; Yang, P.; Liu, J. *J. Am. Chem. Soc.* **2004**, *126*, 1195−1198.

(31) Chen, J.-H.; Tai, M.-F.; Chi, K.-M. *J. Mater. Chem.* **2004**, *3*, 296−298.

(32) Kelly, A. T.; Rusakova, I.; Ould-Ely, T.; Hofmann, C.; Lüttge, A.; Whitmire, K. H. *Nano Lett.* **2007**, *7*, 2920−2925.

(33) Hoefelmeyer, J. D.; Niesz, K.; Somorjai, G. A.; Tilley, T. D. *Nano Lett.* **2005**, *5*, 435−438.

(34) Humphrey, S. M.; Gras, M. E.; Habas, S. E.; Niesz, K.; Somorjai, G. A.; Tilley, T. D. *Nano Lett.* **2007**, *7*, 785−790.

(35) Zettsu, N.; McLellan, J. M.; Wiley, B.; Yin, Y.; Li, Z.-Y.; Xia, Y. *Angew. Chem., Int. Ed.* **2006**, *45*, 1288−1292.

(36) Park, K. H.; Jang, K.; Kim, H. J.; Son, S. U. *Angew. Chem., Int. Ed.* **2007**, *46*, 1152−1155.

(37) Song, H.; Kim, F.; Connor, S.; Somorjai, G. A.; Yang, P. *J. Phys. Chem. B* **2005**, *109*, 188−193.

(38) (a) Khanna, P. K.; Eum, M.-S.; Jun, K.-W.; Baeg, J.-O.; Seok, S. I. *Mater. Lett.* **2003**, *57*, 4617−4621. (b) Oyama, S. T. *J. Catal.* **2003**, *216*, 343−352.

(39) (a) Perera, S. C.; Fodor, P. S.; Tsoi, G. M.; Wegner, L. E.; Brock, S. L. *Chem. Mater.* **2003**, *15*, 4034−4038. (b) Boyanov, S.; Bernardi, J.; Gillot, F.; Dupont, L.; Womes, M.; Trascon, J.-M.; Monconduit, L.; Doublet, M.-L. *Chem. Mater.* **2006**, *18*, 3531−3538.
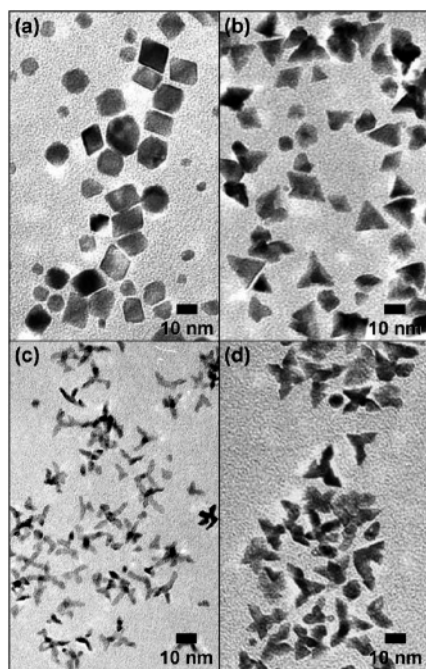
Figure 1. TEM images of Rh nanocrystals used as precursors: (a) cube derivatives (including cubes and octahedra); (b) triangle derivatives (including twinned and etched triangles); (c) thin-armed multipods; (d) thick-armed multipods.
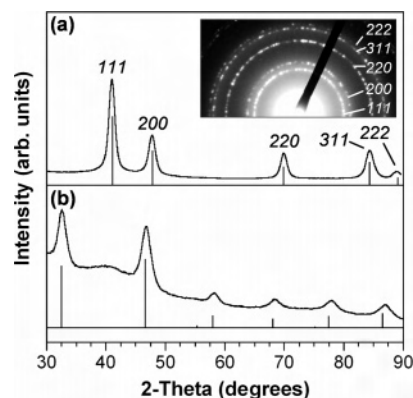
Rh₂P is a known superconductor (T_c = 1.3 K).[40] While we have not probed the low-temperature electronic and magnetic properties of the shape-controlled Rh₂P nanocrystals, it is reasonable to anticipate that advances in the shape-controlled synthesis of this and related functional solids as high-quality single-domain nanocrystals will provide the materials necessary in the future for advanced physical property studies in the nanometer size regime.

Experimental Section

Chemicals. Rhodium(III) chloride hydrate (99.99%, RhCl₃·xH₂O), silver(I) nitrate (99.9%, AgNO₃), poly(vinylpyrrolidone) (40 000 MW, PVP), ethylene glycol (99%, EG), tri-*n*-octylphosphine (tech 90%, TOP), tri-*n*-octylphosphine oxide (98%, TOPO), and oleic acid (tech) were used as purchased from Alfa Aesar. Sodium hexachlororhodate(III) (Na₃RhCl₆), oleylamine (tech 70%), and octyl ether (99%) were used as purchased from Aldrich.

Characterization. Powder X-ray diffraction was performed on a Bruker-AXS GADDS diffractometer using microdiffraction techniques as previously described.[41] Electron microscopy and electron diffraction were performed on a JEOL JEM-2010 transmission electron microscope. Energy dispersive spectroscopy (EDS) was performed using an Oxford Instruments INCA Energy TEM system.

Synthesis of Rh Nanocrystals. Rh Cubes and Octahedra. Rh cubes and octahedra (collectively referred to as "cube-derived nanocrystals") were synthesized using a modification of a method reported by Yang and co-workers for synthesizing Pd and Pt nanocubes in air.[37] (Rh nanocrystals have not previously been reported using this procedure.) A 0.5 mL volume of a 0.002 M

(40) Raub, C. J.; Zachariasen, W. H.; Geballe, T. H.; Matthias, B. T. *J. Phys. Chem. Solids* **1963**, *24*, 1093−1100.
(41) (a) Bhuvanesh, N. S. P.; Reibenspies, J. H. *J. Appl. Crystallogr.* **2003**, *36*, 1480−1481. (b) Bhuvanesh, N. S. P.; Reibenspies, J. H.; Zhang, Y.; Lee, P. L. *J. Appl. Crystallogr.* **2005**, *38*, 632−638.

Figure 2. Powder XRD patterns for representative (a) Rh nanocrystal precursors (PDF card no. 5−0685) and (b) Rh₂P products (PDF card no. 77−0300). A representative SAED pattern for the Rh nanocrystal precursors is shown in the inset.

solution of AgNO₃ in EG was added to 2.50 mL of EG and heated to 190 °C. A 36.1 mg amount of Na₃RhCl₆ in 1.50 mL of EG and 125.2 mg of PVP in 3.00 mL of EG was slowly and simultaneously injected into the Ag⁺/EG solution over 16 min. The reaction was heated for 5 additional min at 190 °C and then cooled to room temperature. The volume of the reaction solution was quadrupled with acetone and centrifuged at 5000 rpm. The precipitate was discarded. The supernatant was collected, its volume tripled with 3:1 hexanes:ethanol, and centrifuged again at 3000 rpm to isolate cube-shaped particles.

Rh Nanocrystal Seeds. Rh nanocrystal seeds were synthesized using a modification of a method reported by Tilley, Somorjai, and co-workers for synthesizing 5.5 nm seeds.[33] A 10.0 mg amount of RhCl₃·xH₂O and 50.0 mg of PVP in 1.00 mL of EG was rapidly injected into 4.0 mL of EG at 190 °C in air. The reaction was heated for 1 h at 190 °C. The solution was cooled to room temperature, and an aliquot was used in the synthesis of Rh triangles. TEM micrographs (Figure S1, Supporting Information) revealed that the seeds had an oblong morphology.

Rh Triangles. Rh triangle and triangle derivatives (twinned and etched triangles) were prepared based on methods reported by Tilley, Somorjai, and co-workers for synthesizing Rh multipods from Rh seeds in air.[33] A 1.00 mL volume of Rh seed nanocrystals was added to 1.00 mL of EG and heated to 140 °C. An 18.9 mg amount of RhCl₃·xH₂O and 50.0 mg of PVP in 1.00 mL of EG was slowly injected into the EG/Rh seed solution at 140 °C over 5 min. The reaction was heated for 5 additional min at 140 °C and then cooled to room temperature. The particles were precipitated by doubling the volume of the solution with acetone. The particles were isolated by centrifugation and then washed with acetone and small amounts of ethanol in acetone.

Rh Multipods (Thin Arms). Rh multipods with thin arms were synthesized by modifying a method reported by Tilley, Somorjai, and co-workers.[33] An 18.9 mg amount of RhCl₃·xH₂O in 0.80 mL of EG and 52.0 mg of PVP in 0.80 mL of EG were slowly and simultaneously injected into 2.00 mL of EG at 110 °C over 5 min in air. The reaction was heated at 110 °C for 5 additional min and then cooled to room temperature. The volume was doubled with acetone to precipitate particles. The particles were isolated by centrifugation and then washed with small amounts of ethanol in acetone.

Rh Multipods (Thick Arms). Rh multipods with thick arms were synthesized according to the procedure reported by Xia and co-workers,[35] except that 40K MW PVP was used instead of 55K.

Conversion of Rh to Rh₂P. Rh₂P Cubes. Rh₂P cubes were synthesized by dispersing 1.4 mg of Rh cube-derived nanocrystals
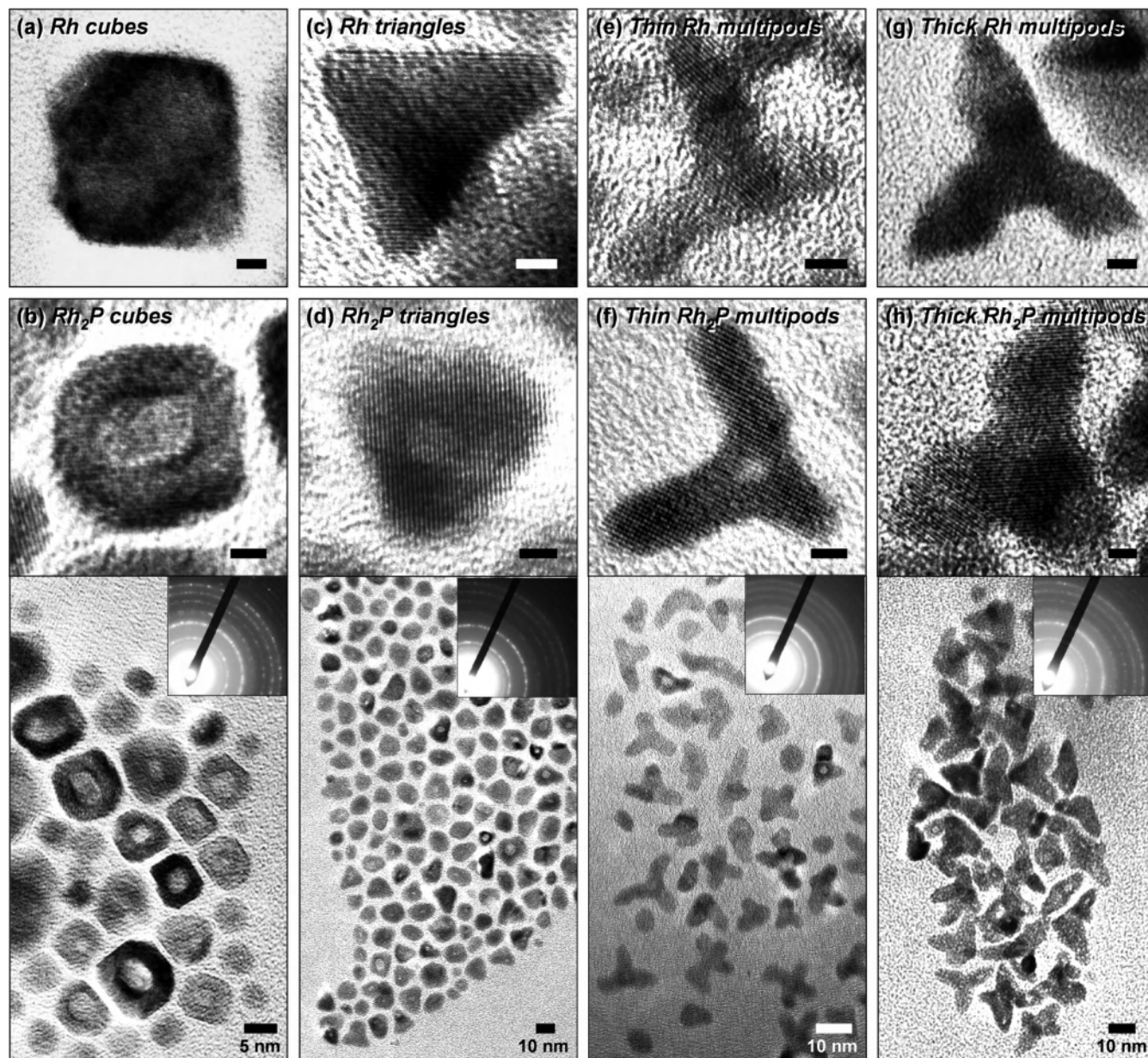
Figure 3. TEM images highlighting the shape-controlled conversion of Rh nanocrystal templates to Rh_2P: (a) Rh cube-derived nanocrystals and (b) Rh_2P formed from (a); (c) Rh triangle-derived nanocrystals and (d) Rh_2P triangles formed from (c); (e) thin-armed Rh multipods and (f) Rh_2P multipods formed from (e); (g) thick-armed Rh multipods and (h) Rh_2P multipods formed from (g). Scale bars are 2 nm unless otherwise labeled.

into 1.0 mL of TOP with 0.25 mL of ethanol and 0.500 mL of oleylamine. This solution was injected into 1.0 g of TOPO at 360 °C under Ar and aged for 1 h after injection at 330 °C. After the reaction was cooled, it was saturated with ethanol and centrifuged at 13K rpm. The isolated particles were washed with ethanol and small amounts of hexanes and then dried under Ar.

Rh_2P Triangles. Rh_2P triangles were synthesized by dispersing 2.0 mg of Rh triangle-derived nanocrystals into 1.0 mL of TOP with 0.50 mL of oleylamine. This solution was injected into 1.0 g of TOPO at 360 °C under Ar and aged for 1 h at 360 °C. The reaction was cooled and the particles isolated and washed as described above.

Rh_2P Multipods (Thin Arms). Rh_2P multipods with thin arms were synthesized by dispersing 1.5 mg of Rh multipods (thin arms) in 1.0 mL of TOP with 0.50 mL of ethanol and 0.50 mL of octyl ether. This solution was injected into 1.0 g of TOPO at 360 °C under Ar and then aged for 1 h after injection, eventually reaching

360 °C. The solution took approximately 20 min to return to 360 °C, because injecting a substantial amount of ethanol decreased the temperature instantly ($\sim$320 °C). After 1 h, the reaction was cooled and the particles were isolated and washed as described above.

Rh_2P Multipods (Thick Arms). Rh_2P multipods with thick arms were synthesized using Rh multipods that had been mixed with oleylamine immediately after their synthesis. A 4.7 mg amount of Rh multipods (thick arms) was dispersed in 1.0 mL of TOP. This solution was injected into 1.0 g of TOPO at 360 °C under Ar and then aged for 1 h at 340 °C. The reaction was cooled, and the particles were isolated and washed as described above.
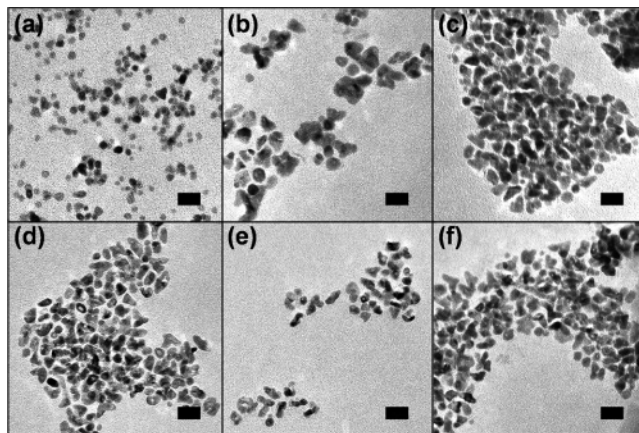
Results and Discussion

Like other transition metals that crystallize in an fcc structure, rhodium can form nanocrystals with various
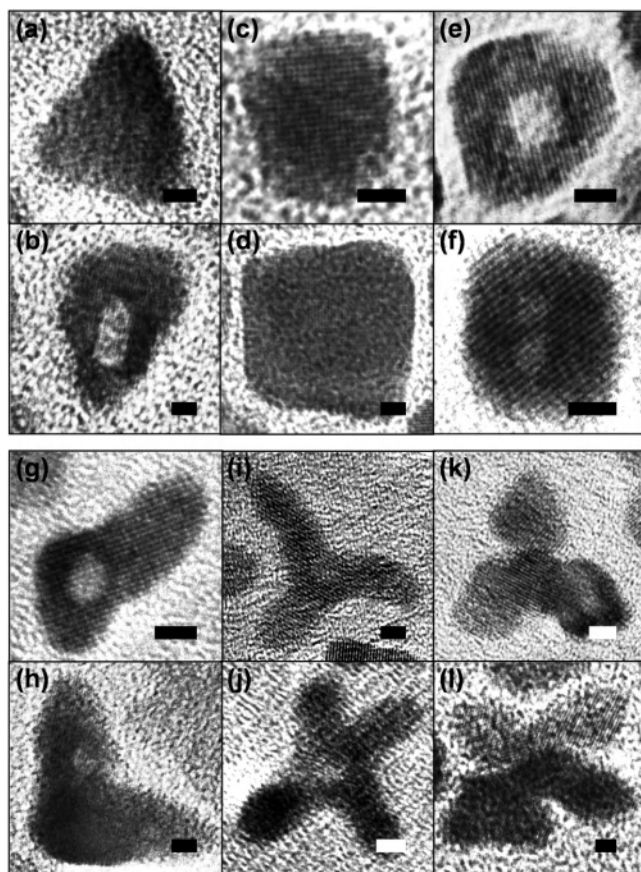
Figure 4. Representative Rh₂P nanostructures obtainable by reaction of Rh nanocrystals with TOP: (a) solid triangle; (b) hollow triangle; (c, d) solid cubes; (e, f) hollow cubes; (g, h) fractured multipods; (i, j) multipods with hollow cores; (k, l) multipods with hollow arms. All scale bars are 2 nm.

Figure 5. Rh₂P multipods made with various cosolvents, injected, and aged for 1 h at 360 °C unless otherwise noted: (a) oleic acid; (b) octyl ether; (c) oleylamine; (d) ethanol + oleylamine (aged 15 min); (e) ethanol; (f) ethanol (aged at 340 °C). All scale bars are 20 nm.

morphologies.[33−37] The formation of regular polyhedral nanocrystals is influenced by the stabilizing polymer PVP, poly(vinylpyrrolidone), as has been seen for other metals such as Au, Pd, Pt, and Ag.[7] By variation of the Rh^{3+}:PVP ratios, the reaction temperature, and the Rh^{3+} precursor, four separate nanocrystal morphologies can be accessed, as seen in the transmission electron micrographs (TEM) in Figure 1. Cube-derived Rh nanocrystals, which collectively include a variety of single-crystal cubes and octahedra (Figure 1a), can be made by modifying a previously reported method for making Pd and Pt nanocubes.[37] Similarly, Rh triangle derivatives, including single-crystal and multiply twinned triangles and tetrahedra (Figure 1b), can be formed when Rh seed crystals are used.[33] Rh multipods, which are a mixture of tripods and tetrapods, can be made in two different ways. The first method, based on a modification of work reported by Tilley, Somorjai, and co-workers[33] using $RhCl_3$ as the Rh^{3+} source, results in multipods with long, thin arms that grow around a spherical core (Figure 1c). The second method, developed by Xia and co-workers,[35] utilizes Na_3-$RhCl_6$ as the Rh^{3+} source and results in single-crystal tripods and tetrapods (Figure 1d) with arms that have varying thickness as they branch out from the center. For each morphology of Rh nanocrystals, the samples are phase pure (fcc Rh) by powder X-ray diffraction and selected area electron diffraction (SAED, Figure 2). These four distinctive

shapes of Rh nanocrystals, which we can synthesize with roughly the same level of shape purity that has been reported in the literature (see Supporting Information for statistical analysis), can serve as templates for conversion into Rh₂P. The morphology of the Rh₂P product is defined by the morphology of the Rh nanocrystal templates.

In a typical reaction to convert a metal nanocrystal to a metal phosphide, the metal nanocrystals are dispersed in TOP and injected into a hot, coordinating solvent, such as trioctylphosphine oxide (TOPO), under argon.[24,25] It is understood that colloidal metals can induce cleavage of the P−C bond in alkylphosphines creating a reactive phosphorus species,[42] although, within the context of these TOP/metal nanoparticle reactions, byproducts have not yet been isolated and characterized. A similar reaction can be used to convert the Rh cubes/octahedra, triangles and multipods into Rh₂P, which is verified by XRD (Figure 2). A small amount of nanocrystalline Rh is evident in the XRD pattern for Rh₂P, likely from some unreacted Rh (discussed later). As shown in Figure 3, cube-derived Rh nanocrystals (Figure 3a) form both solid and hollow single-crystal Rh₂P cubes (Figure 3b, ∼50% hollow). There is a substantial amount of shape conservation, with ∼75% of the cube-derived Rh nanocrystal precursors (cubes and octahedra) maintaining a cube-derived shape upon conversion to Rh₂P. Rh nanocube size seems to be largely responsible for generating hollow vs dense nanocubes, which is consistent with previous observations of size-dependent hollowing for the conversion of spherical Ni nanocrystals to Ni₂P.[24] However, this is not absolute—a few hollow and dense nanocubes of the same size are sometimes found. In the case of Rh₂P, nanocubes larger than 7−8 nm tend to be hollow, while smaller ones tend to be dense. Similar to the cubes, triangle-shaped Rh nanocrystals (Figure 3c) convert to Rh₂P triangles (Figure 3d) by reaction with hot TOP. Although 40% of the triangle-derived Rh₂P

(42) (a) Chen, J.-H.; Tai, M.-F.; Chi, K.-M. *J. Mater. Chem.* **2004**, *14*, 296−298. (b) Schmidt, F. K.; Belykh, L. B.; Cherenkova, T. V. *Kinet. Catal.* **2001**, *42*, 163−173. (c) Khanna, P. K. P. K.; Jun, K.-W.; Hong, K. B.; Baeg, J.-O.; Mehrotra, G. K. *Mater. Chem. Phys.* **2005**, *92*, 54−58.

Table 1. Effects of Cosolvents on the Quality of Rh$_2$P Multipods

cosolvent combination	extent of Rh dispersability (PVP-stabilized multipods)[a]	morphological retention of Rh$_2$P[b] (%) (temp, °C)
ethanol[c] + TOP	heterogeneous solution (emulsion), visible particulates	49 (360), 60 (340)
oleic acid + TOP	homogeneous solution	7
oleylamine + TOP	heterogeneous solution (emulsion), visible particulates	55 (360), 72 (340)
octyl ether + TOP	heterogeneous solution, large aggregated particulates	15
ethanol + octyl ether + TOP	heterogeneous solution, visible particulates	48
ethanol + oleylamine + TOP	slightly turbid, no visible particulates	28 (360), 62 (340)

[a] Dispersability of PVP-stabilized Rh multipods is related to the solubility of PVP in the given solvents. [b] Morphological retention is based on the percentage of Rh$_2$P particles retaining their original multipod (tetrapod or tripod) shape: % multipods for Rh$_2$P product/% multipods in Rh precursor. A total of 150−400 particles were categorized for each sample, depending on image quality. No aggregated particles were included since edges and faces could not be clearly discerned. Data are given for conversion reactions aged at 360 °C for 1 h unless otherwise noted. [c] Ethanol is presumed to vaporize instantly upon injection at the high reaction temperatures.

nanostructures are hollow, they tend to have slightly rounded corners and, in some cases, lose their triangular shape completely.

Reaction of Rh multipods with TOP results in Rh$_2$P multipods with distinct morphological characteristics that are templated by the precursor nanocrystals (Figure 3e−h). For the long, thin-armed Rh multipod precursors (Figures 1c and 3e), the Rh$_2$P products (Figure 3f) maintain the shape of the Rh precursors, including many that show hollow cores but not hollow arms. This is likely a size effect, since the arms are narrower than the core. Loss of multipod arms was often observed in the Rh$_2$P products, presumably due to the harsh conditions of the conversion reaction and the fragility of the multipod arms. In contrast to the Rh$_2$P multipods with long, thin arms, the multipods with thicker arms (Figure 3g) were hollow only in the arms and not the core (Figure 3h). In this case, the arms are more accessible and the cores are hindered by the bulky arms, so diffusion of P into the Rh arms is likely to occur more readily.

Figure 4 shows representative examples of the types of Rh$_2$P nanocrystals that can be generated via reaction of Rh nanocrystals with TOP, including the range of branched Rh$_2$P nanocrystals that are observed (monopods, bipods, tripods, and tetrapods). Rh$_2$P cubes, triangles, and multipods are accessible as both hollow and dense nanocrystals. Generally the ability to access hollow vs dense nanostructures is related to the size of the precursor nanocrystals, as well as temperature. Both of these factors influence diffusion, which is responsible for the formation of Kirkendall-mediated voids.[43] It is important to note that our Rh nanocrystal precursors are of quality (size, uniformity, shape purity) similar to those reported in the literature (see Supporting Information for statistical analysis).[33−36] For example, our ability to generate Rh multipod samples containing mixtures of tripods and tetrapods, as well as bent, linear, and spherical nanostructures, mimics literature reports using similar procedures.[33−36] In general, the relative populations of each of the morphologies in the final Rh$_2$P products are close to those in the Rh precursors as discussed earlier, with some additional degradation caused by the reaction with TOP. If one could synthesize Rh nanocrystal samples with better monodispersity and shape purity than is currently achievable using available literature methods, it is likely that nearly shape-pure samples of Rh$_2$P nanocrystals could be generated, as well as samples that are entirely hollow or dense.

For fcc metals such as Rh, it is known that the (111) planes have the lowest surface energy, followed by (100) and (110).[44] The relationship between surface energy and the shape of Rh nanocrystals has been discussed in depth in the literature.[33,35,44] In general, shapes that deviate from the thermodynamically favored truncated octahedron geometry are kinetically controlled and accessible because of the presence of surface stabilizers or the use of seeded growth strategies. To our knowledge, the relative surface energies for Rh$_2$P are not known. However, the formation of Rh$_2$P nanocrystals with a variety of different nanocrystal morphologies, and therefore different exposed crystal planes, implies that at least some are kinetically controlled. This, in turn, implies that these same surface stabilizers (which remain present throughout the conversion from Rh to Rh$_2$P) similarly stabilize the Rh$_2$P surfaces. This is reasonable considering the diffusion-based reaction of P (from TOP) with the Rh nanocrystals and the relationship between the crystal structures of Rh and Rh$_2$P,[45] which likely minimizes major morphological changes. However, truncated edges and corners are frequently observed in the Rh$_2$P nanocrystals. For example, the Rh$_2$P hollow cubes show lattice spacings corresponding to the (200) planes and frequently show truncated corners corresponding to the (111) planes. This suggests competition between the relative stabilities of the Rh$_2$P planes and those of the precursor Rh nanocrystals.

To guarantee the shape-controlled conversion of the Rh nanocrystals to Rh$_2$P, there are a few crucial issues that need to be addressed. In contrast to previous reports of metal-to-metal phosphide conversion reactions that use hexadecylamine- or oleylamine-stabilized metal nanocrystals[24−26] that are soluble in TOP, the PVP-stabilized particles are immiscible with TOP. Since PVP is responsible for controlling the shape of the Rh nanocrystals,[7] stabilizing ligands that show good miscibility with TOP (such as amines or other ligands and surfactants) are not easily substituted for PVP. However, the PVP coating the nanocrystal surface, which

(43) (a) Smigelskas, A. D.; Kirkendall, E. O. *Trans. AIME* **1947**, *171*, 130−142. (b) Fan, H. J.; Knez, M.; Scholz, R.; Hesse, D.; Nielsch, K.; Zacharias, M.; Gösele, U. *Nano Lett.* **2007**, *7*, 993−997.

(44) (a) Wen, Y.-N.; Zhang, J.-M. *Solid State Commun.* **2007**, *144*, 163−167. (b) Zhang, J.-M.; Ma, F.; Xu, K.-W. *Appl. Surf. Sci.* **2004**, *229*, 34−42. (c) Vitos, L.; Ruban, A. V.; Skriver, H. L.; Kollár, J. *Surf. Sci.* **1998**, *411*, 186−202.

(45) (a) Ross, R. G.; Hume-Rothery, W. *J. Less-Common Met.* **1963**, *5*, 258−270. (b) Zumbusch, M. *Z. Anorg. Chem.* **1940**, *243*, 322−329. (c) Rundqvist, S. *Nature* **1960**, *185*, 31−32. (d) Secoue, M.; Auvray, P.; Toudic, Y.; Ballini, Y. *J. Cryst. Growth* **1986**, *76*, 135−141.

defines its solubility, can be coated with cosolvents that help to bridge the miscibility gap between PVP and TOP. This effectively increases the ability to disperse the Rh nanocrystals in TOP and also minimizes degradation of the nanocrystal shape during the conversion reaction. Ethanol, oleic acid, oleylamine, and octyl ether are potential cosolvent candidates because they demonstrate sufficient miscibility with TOP, and PVP-coated nanocrystals are somewhat dispersible in them (see Supporting Information).

Combinations of these cosolvents could also be used to fine-tune the particle/solvent interactions and possibly facilitate enhanced shape conservation via improved dispersion and shape retention. For example, adding oleic acid to the Rh−TOP solution creates a visibly homogeneous solution. However, as shown for the case of thin-arm Rh multipods dispersed with oleic acid in TOP, the resulting Rh₂P particles are largely spherical (Figure 5a). Specifically, 93% of the Rh₂P products are spherical, compared to only 38% when using optimal conditions (e.g., those used to generate the products shown in Figure 3f). In this case, the cosolvent aides miscibility but destroys the morphology of the template. In contrast, using oleylamine, octyl ether, and ethanol (and combinations of them) as cosolvents results in improved shape conservation in the Rh₂P product (Figure 5b−f), as detailed in Table 1. Despite this, a truly homogeneous solution of the PVP-stabilized particles and TOP cannot be obtained, but the conversion reaction can still proceed with reasonably good morphology retention. Table 1 summarizes the ability of various combinations of cosolvents to facilitate the shape-controlled conversion of Rh nanocrystals into Rh₂P via reaction with TOP, as shown in the TEM micrographs in Figure 5. In general, the highest quality Rh₂P nanocrystals are generated using solvent mixtures that include oleylamine and TOP and temperatures that are on the lower end of those used in nanocrystal/TOP reactions (∼340 °C).

As is evident from the observations included in Table 1, temperature also plays a key role in optimizing shape retention and product purity, as well as the ability to generate hollow nanostructures. When Rh nanocrystals dispersed in TOP are injected at 360 °C and aged at that temperature for 1 h, phase-pure Rh₂P (by powder XRD, not shown) is always obtained, and the product usually has a high percentage of hollow particles, regardless of morphology. However, the high reaction temperature can result in Rh₂P nanocrystals that have lost their original shape and are highly aggregated. When the injection temperature is 360 °C but the aging temperature is lowered to 330−340 °C, a higher degree of shape conservation is observed, though there are considerably fewer hollow particles. For example, when oleylamine is used as a cosolvent, there is a significant improvement in Rh₂P shape quality if the reaction is aged at 340 °C (Figure 3h, 62% shape retention) vs 360 °C (Figure 5c, 28% shape retention). However, the improved shape quality is at the cost of product purity. At lower temperatures, the Rh₂P

products retain their shape reasonably well, but some unreacted Rh remains, as seen by powder XRD (Figure 2b) and EDS (not shown, ∼5−10% increase in Rh content relative to P compared to product aged at 360 °C). These observations imply that higher aging temperatures facilitate complete conversion of Rh to Rh₂P, show less ability to retain the shape of the Rh precursors (spherical shapes are preferred), and favor hollow nanostructures. Likewise, lower aging temperatures (330−340 °C) tend to result in incomplete conversion (e.g., Rh impurities remain), maintain the shape of the Rh precursors, and generate dense nanostructures. Consistent with this, the optimal reaction conditions for maintaining the regular multipod shape (Figure 3h) while maximizing conversion efficiency are to inject the Rh−TOP solution at 360 °C and age at 340 °C for 1 h. The window of optimal conditions for generating the highest quality Rh₂P nanocrystals is narrow but achievable and points to the critical roles that the key synthetic variables have on ensuring shape-controlled conversion of a metal nanocrystal into a metal phosphide.

Conclusions

In this paper, we described the shape-controlled conversion of a diverse library of Rh nanocrystal shapes into dense and hollow Rh₂P nanocrystals, which represents the most morphologically diverse set of metal phosphide nanocrystals reported to date. Our studies also provide insights into shape-controlled nanocrystal conversion reactions that are likely to be applicable to other phosphide and multielement nanocrystal systems. This is important because it is rapidly becoming straightforward to control the quality, shape, and uniformity of single-metal nanocrystals[7−8] but similar achievements (and general synthetic strategies) for multimetal nanostructures are less common. Employing, understanding, and optimizing template-based strategies provides an alternative mechanism for increasing the complexity of solid-state materials that are accessible as well-controlled nanocrystals.

Supporting Information Available: TEM image of Rh seed nanocrystals, tables summarizing solvent miscibility and nanocrystal dispersability, a statistical analysis of Rh nanocrystal shapes, and views of the crystal structures of Rh and Rh₂P. This material is available free of charge via the Internet at http://pubs.acs.org.

IC701783F